

UC San Diego

UC San Diego Previously Published Works

Title

Coordination of gene expression with cell size enables Escherichia coli to efficiently maintain motility across conditions

Permalink

<https://escholarship.org/uc/item/5hz5f714>

Journal

Proceedings of the National Academy of Sciences of the United States of America, 119(37)

ISSN

0027-8424

Authors

Honda, Tomoya
Cremer, Jonas
Mancini, Leonardo
et al.

Publication Date

2022-09-13

DOI

10.1073/pnas.2110342119

Peer reviewed



Coordination of gene expression with cell size enables *Escherichia coli* to efficiently maintain motility across conditions

Tomoya Honda^{a,b,1}, Jonas Cremer^{c,d,1}, Leonardo Mancini^{e,f}, Zhongge Zhang^a, Teuta Pilizota^e, and Terence Hwa^{a,c,2}

Edited by Seppe Kuehn, The University of Chicago, Chicago, Illinois; received June 4, 2021; accepted August 4, 2022 by Editorial Board Member Thomas J. Silhavy

To swim and navigate, motile bacteria synthesize a complex motility machinery involving flagella, motors, and a sensory system. A myriad of studies has elucidated the molecular processes involved, but less is known about the coordination of motility expression with cellular physiology: In *Escherichia coli*, motility genes are strongly up-regulated in nutrient-poor conditions compared to nutrient-replete conditions; yet a quantitative link to cellular motility has not been developed. Here, we systematically investigated gene expression, swimming behavior, cell growth, and available proteomics data across a broad spectrum of exponential growth conditions. Our results suggest that cells up-regulate the expression of motility genes at slow growth to compensate for reduction in cell size, such that the number of flagella per cell is maintained across conditions. The observed four or five flagella per cell is the minimum number needed to keep the majority of cells motile. This simple regulatory objective allows *E. coli* cells to remain motile across a broad range of growth conditions, while keeping the biosynthetic and energetic demands to establish and drive the motility machinery at the minimum needed. Given the strong reduction in flagella synthesis resulting from cell size increases at fast growth, our findings also provide a different physiological perspective on bacterial cell size control: A larger cell size at fast growth is an efficient strategy to increase the allocation of cellular resources to the synthesis of those proteins required for biomass synthesis and growth, while maintaining processes such as motility that are only needed on a per-cell basis.

bacterial chemotaxis | cell size | gene expression | growth physiology | growth-rate control

To thrive in different environments, bacteria must efficiently allocate their limited resources toward different cellular processes in accordance to what is most needed for their growth and survival (1). Flagella-driven motility is one of the most distinct processes of bacterial life that provides cells with novel ways to respond to the conditions they encounter (2). The active movement toward more favorable conditions and away from detrimental ones has been studied in detail on the molecular level (3–5) and can give rise to strong fitness advantages (6–9). However, flagella-driven motility is also a resource-demanding process. For growing *Escherichia coli* cells, the synthesis of the motility proteins alone ties up a substantial portion of the protein synthesis resources (10, 11), and the assembly and rotation of flagella also demand energy (12–14). Accordingly, motility expression constitutes a burden on cell growth, such that cells with attenuated motility can grow up to 20% faster and reach about 10% higher biomass yields (15–17), a strong difference readily affecting the outcome of (laboratory) evolution (18–21). Given this burden, the expression of motility is expected to be highly controlled, in coordination with other cellular processes and demands (22–25).

Notably, the expression of motility genes varies strongly with the nutrient conditions cells encounter, and more resources are allocated to motility expression in nutrient-poor than in replete conditions (26–30). These observations have been taken as support for the idea that motility is a response expressed to search for alternative nutrient sources when local nutrient sources are depleted (26, 29, 30). However, swimming speeds observed during balanced growth do not vary much with the growth rate or the carbon source provided (9). Furthermore, bacterial populations exhibit a chemotaxis-driven form of range expansion (6, 8, 31–33), with expansion speeds that are markedly faster in nutrient-replete conditions providing faster growth (9). These latter observations suggest that motility is a phenotype broadly expressed by growing cells, rather than merely being a foraging response to starvation. However, why then are motility genes expressed more highly in poor growth conditions, and how does their degree of expression affect swimming? To resolve this puzzle, we systematically investigated the link between gene expression and swimming in different balanced growth conditions. We found that *E. coli* K-12 cells coordinate their

Significance

To swim, bacteria must regulate a battery of motility genes in proper relation to other genes and the environments they encounter. To reveal how cells resolve this challenge, we studied the regulation of motility genes in the model organism *Escherichia coli* across growth conditions. By connecting gene expression with swimming behavior and growth, we illustrate how cells coordinate the regulation of swimming machinery with cell size such that the number of flagella per cell is maintained across conditions. The findings revise previous interpretations that saw swimming motility as a starvation response. Instead, cells are motile across growth conditions with size-dependent regulation, ensuring an efficient allocation of cellular resources to the synthesis of costly flagella machinery.

Author contributions: T. Honda, J.C., T.P., and T. Hwa designed research; T. Honda, J.C., L.M., and Z.Z. performed research; Z.Z. contributed new reagents/analytic tools; T. Honda, J.C., L.M., T.P., and T. Hwa analyzed data; and T. Honda, J.C., and T. Hwa wrote the paper.

The authors declare no competing interest.

This article is a PNAS Direct Submission. S.K. is a guest editor invited by the Editorial Board.

Copyright © 2022 the Author(s). Published by PNAS. This open access article is distributed under Creative Commons Attribution-NonCommercial-NoDerivatives License 4.0 (CC BY-NC-ND).

¹T.H. and J.C. contributed equally to this work.

²To whom correspondence may be addressed. Email: hwa@ucsd.edu.

This article contains supporting information online at <http://www.pnas.org/lookup/suppl/doi:10.1073/pnas.2110342119/-DCSupplemental>.

Published September 6, 2022.

gene expression with cell size to maintain motility; the up-regulation of motility genes at slower growth is a necessary compensation to adjust for growth-related changes in cell size such that the number of flagella per cell remains constant. This simple regulatory objective provides an example of how cells can maintain a function while keeping resource demands minimal. Our findings also provide a perspective on the relation between cell size control and proteome resource allocation, giving a physiological rationale for the ubiquitously observed positive relation between cell growth and cell size.

To study the relation between swimming behavior and motility gene expression, we first examined gene expression during balanced growth across a broad range of growth conditions, using a physiologically well-characterized strain (wild-type [WT] strain *E. coli* K-12 HE204; *SI Appendix, Text 1.1*). Motility genes are hierarchically regulated and have been assigned into three different classes, with the master regulator *flhDC* being the class I genes as illustrated in *SI Appendix, Fig. S1A* (22–24). We first studied the expression of *fliA*, a class II gene that encodes the sigma factor σ_F required for the expression of flagella components (class III genes). Using a LacZ reporter (strain HE207), we quantified the expression level of the *fliA* promoter (in unit of LacZ activity per biomass; *SI Appendix, Text 1.4*) during balanced growth, with a range of growth rates obtained by supplementing minimal medium with different carbon sources or rich media components (detailed growth conditions are described in *SI Appendix, Text 1.2*). Consistent with previous reports (26, 28–30), *fliA* expression was higher at slower growth rates (Fig. 1*A*, circles): Expression levels changed approximately exponentially with growth rate (dashed line), with an ~ 4.4 -fold increase when growth rates changed from fast (1.60 1/*h* for growth on rich defined medium [RDM] with glucose) to slow (0.28 1/*h* for growth on aspartate). The same trend was observed for the abundance of FliA and other class II proteins, including the hook-basal body components, as supported by available proteomics data (11) (*SI Appendix, Fig. S1 B and C*). We next studied the promoter activities of a class I and a class III gene using LacZ reporters. Expression of the master regulator gene *flhD* (class I) and the flagellin-encoding gene *fliC* (class III) also showed similar changes to the *fliA* promoter activity (class II) (*SI Appendix, Fig. S1 D and E*). The fold change is distinct from a constitutively active promoter, *P_{tet}-lacZ*, that showed significantly less variation in the activity (*SI Appendix, Fig. S2 A and D*). We also verified that the replacement of the native 5′-untranslated region (UTR) in *flhD* with the synthetic *lacZ* UTR results in a significantly reduced fold change of *flhD* expression (*SI Appendix, Fig. S2 B and D*), capturing the importance of posttranscriptional regulation (34, 35). In summary, these data suggest that cells express motility genes in a growth-dependent manner and the master regulator *flhDC* plays a key regulatory role for the overall expression.

The observed growth-dependent expression provides a substantial growth rate–dependent burden for the cell. Particularly, a deletion of the master regulator *flhD*, which results in the complete suppression of motility gene expression, increased growth rate by up to 18% compared to the WT strain, with larger increases realized in slower growth conditions where motility expression in the WT was higher (*SI Appendix, Fig. S2E*). To rationalize this costly expression and understand its relation to the motile phenotypes, we next characterized swimming behavior in different growth conditions. Extending a previous approach combining phase-contrast microscopy and tracking (9), we quantified the movement of hundreds of cells and analyzed the distributions of observed swimming speeds $\{v_i\}$ during run events (see Fig. 1*B* and *SI Appendix, Fig. S3 and Text 1.3* for methods). We then extracted the average

swimming speed and the fraction of motile cells with swimming velocities $v_i > 5 \mu\text{m/s}$. Notably, despite the ~ 4.4 -fold change of gene expression (Fig. 1*A*), swimming characteristics varied only weakly: The fraction of swimming cells (α_m) remained close to 90% for all growth conditions (Fig. 1*C*), and the average swimming speed, $v = \langle v_i \rangle$, changed only ~ 1.3 -fold from fast (RDM with glucose) to slow (aspartate) growth (Fig. 1*D*).

One possible explanation for this combined observation of minor changes in swimming behavior and large changes in expression of motility genes would be an adjustment to a possible decrease in flagella motor activity at slow growth: The *E. coli* flagella motor is driven by the proton motive force (PMF), and the motor rotation frequency is proportional to the PMF (12, 13). Given that the PMF is a result of the metabolic state, which might change with growth condition, the cell might compensate for slower rotation in poor growth conditions by increasing the expression level of motility genes. To probe this idea, we measured motor activity by tracking the rotation of beads attached to flagella filaments (36, 37). However, the rotation frequency was found to be almost independent of growth (Fig. 1*E*; a drop of 13% from growth rate 0.87 1/*h* to 0.39 1/*h*).

Why then are motility genes expressed more in slow growth conditions? To investigate this question further, we next performed experiments with a synthetic construct that allows for the smooth titration of motility gene expression in a given growth condition so that we could separately assess the effect of changing motility expression and growth. We replaced the native promoter of the master regulator *flhDC* with the *P_{tet}* promoter, enabling an inducer-dependent control. Additionally, the construct also carries the above-mentioned *P_{fliA}-lacZ* as a reporter for class II gene expression (see Fig. 2*A* and *SI Appendix, Text 1.1.3* for cartoon and details). We first grew this strain in fructose minimal medium with different concentrations of the inducer chlortetracycline (cTc). *P_{fliA}-lacZ* expression decreased smoothly from WT levels toward zero when the inducer concentration in the media was reduced (Fig. 2*A*, blue points). Decreasing the inducer concentration similarly shifted the distribution of swimming speeds (Fig. 2*B*) toward lower average swimming speeds and motile fractions (Fig. 2*C and D*, blue points). Similar results were obtained by growing cells in other carbon sources that provide faster and slower growth rates (Fig. 2, glucose and mannose as green and magenta points). Overall, these results show that motility gene expression has a strong influence on cellular swimming behaviors at each growth condition, as can also be seen by directly plotting swimming speed and motility fraction against *fliA* expression (*SI Appendix, Fig. S4*).

To better understand how the regulation of motility genes determines swimming behavior, we next compared how the swimming phenotypes change across growth conditions when motility gene expression remains at a constant level. Using the titratable construct and selected inducer levels, we particularly chose two different expression levels (dotted and dashed lines, Fig. 3*A*). Comparing swimming behavior at these two expression levels, we found a gradual reduction of swimming speed as the growth rate slowed down (Fig. 3*B and C*). This reduction can be largely accounted for by a reduction of the fraction of motile cells (Fig. 3*D*), while the average swimming speed of motile cells remained within narrow ranges (Fig. 3*B*, gray vertical lines). In summary, these observations suggest that the up-regulation of motility genes at slower growth is necessary to keep the population motile but not to increase the swimming speed of the motile cells.

To better understand the regulation of motility genes and its connection to swimming behavior, we next considered the

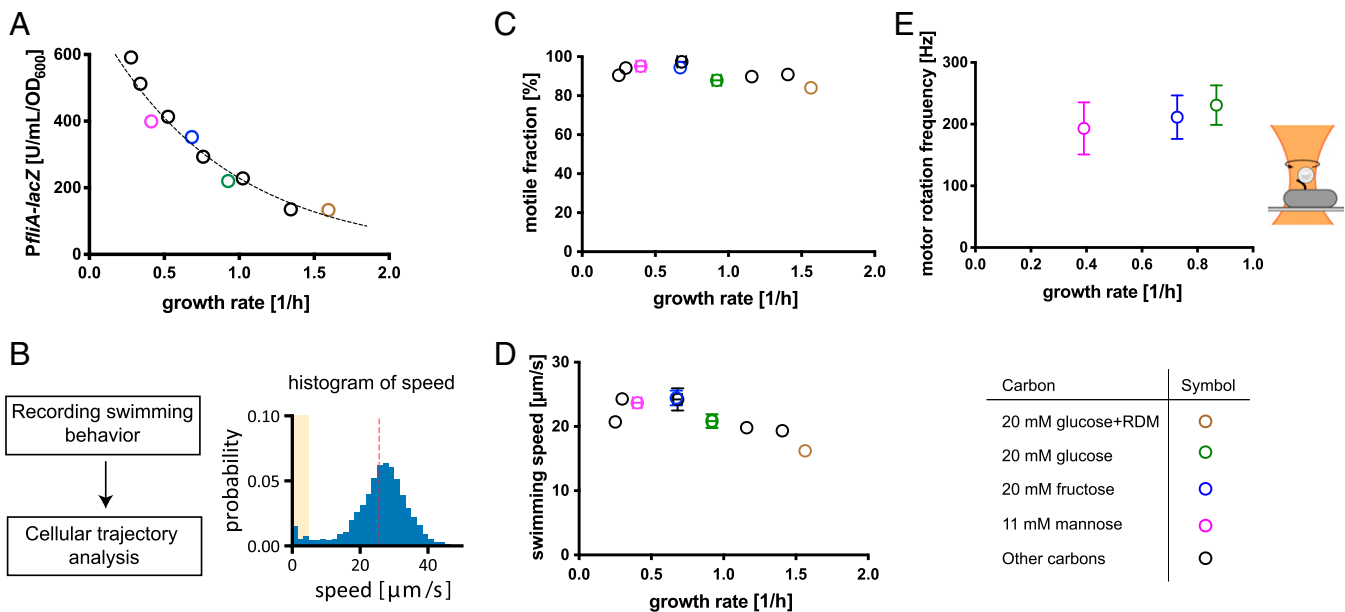


Fig. 1. Motility gene expression and swimming behavior during balanced growth in different growth media. (A) Expression level of a reporter of the *fliA* promoter (a class II gene; *SI Appendix, Fig. S1A*) for growth on different carbon sources (circles). The reporter expression changes strongly with growth rates. Dashed line indicates exponential fit, $734 \cdot e^{-k \cdot \lambda}$ with rate $k = 1.17 \text{ 1/h}$. (B) Quantification of swimming behavior: Using phase-contrast microscopy, cells were tracked and swimming speeds were analyzed (details in *SI Appendix, Text 1.3*). Cell-to-cell variation of swimming speeds for growth on fructose as example. The red line indicates the mean swimming speed, and the yellow background indicates the range, defined as nonmotile (swimming speeds $v_i < 5 \mu\text{m/s}$). Additional conditions and reproducibility are shown in *SI Appendix, Fig. S3*. (C and D) Motile fractions and average swimming speeds for different growth rates, which show minor variations with growth rate. Error bars of SD are provided when biological replicates are available (*SI Appendix, Fig. S3 and Table S6*). (E) Motor rotation frequency for different growth rates. Error bars indicate SD observed for the probed population (*SI Appendix, Table S7*). Rotation frequencies of beads attached to filament stub were measured using back-focal plane interferometry, and a strain with the filament gene was modified to readily stick to polystyrene beads (sticky-*fliC*) (38, 39); see cartoon and *SI Appendix, Text 1.6*. Data in rich media were not collected because rapid cell divisions prevented motor observation for sufficient periods. Four reference conditions are highlighted by colors as indicated in the legend table. Strains HE207, HE206, and HE608 were used in A, C and D, and E, respectively. The data values are listed in *SI Appendix, Tables S2, S6, and S7*.

abundance of motility gene products per cell: Gene expression levels, as those determined via a LacZ reporter, are typically quantified per biomass [e.g., the commonly used “Miller Unit” (40) quantifies LacZ activity per biomass; unit $U/mL/OD_{600}$, with optical density $(OD)_{600}$ having a constant relation with biomass across growth condition (41); *SI Appendix, Texts 1.4 and 2*]. Since these expression levels correlate with protein mass per biomass, as previously discussed (*SI Appendix, Fig. S1*), and biomass itself is proportional to cell volume due to the constancy of biomass density (11, 42), the measurements with the class II gene reporter *PfliA-lacZ* reflect the concentration of class II gene products (flagella hook and basal body; *SI Appendix, Fig. S1* and Fig. 4A, Top row). As confirmed by the LacZ reporters (Fig. 1A and *SI Appendix, Fig. S1 D and E*) and available proteomics data (11) (*SI Appendix, Fig. S1 B and C*), this concentration is higher when cells grow more slowly. However, bacterial cells also have different cell sizes at different growth rates. In fact, the average biomass per cell exhibits an approximate exponential dependence on the growth rate (Fig. 4B), known as the Schaechter-Maaloe-Kjeldgaard relation (43–45). Accordingly, the average abundance of class II gene products per cell is expected to exhibit less change with growth rate than what is observed for the concentration (Fig. 4A, Bottom row). Confirming this idea, the *PfliA-lacZ* expression per cell (unit: $U/cell$), taken as the product of expression per biomass (unit: $U/mL/OD_{600}$) and the average biomass per cell (unit: $mL \cdot OD_{600}/cell$), is nearly independent of growth rate (Fig. 4C, filled red points). Remarkably, the exponential relations observed for cell size (Fig. 4B, dashed line) and the expression level per biomass (Fig. 4C, dashed black line) show similar absolute rates (1.18 h^{-1} and 1.17 h^{-1}), leading to the abundance per cell being independent of growth rate (Fig. 4C, dotted red line).

The above analysis suggests that cells maintain their number of flagella across growth conditions and that the large change of gene expression with growth rate is necessary to keep this number constant as the cell size changes. To confirm this idea more directly, we counted the number of flagella filaments attached to the cells using a staining assay (*SI Appendix, Fig. S5 and Text 1.5*). We confirmed that the average number of flagella filaments per WT cell remained within a narrow range across growth conditions (four or five, within the measurement error) (*SI Appendix, Fig. S5D*). As an example, two cells of different sizes but similar flagella numbers are shown in Fig. 4D. Looking at the distribution of filament numbers across the population, we see that very few cells possess only one or zero filaments (*SI Appendix, Fig. S5B*), consistent with a high fraction of motile cells (Fig. 1C). In contrast, the average number of filaments varied strongly for the titratable *flhDC* strain as the provided inducer concentration was varied (*SI Appendix, Fig. S6*). Particularly, the fraction of cells with zero or one filament clearly increased at lower inducer concentrations (*SI Appendix, Fig. S6 A and B*), which coincides with the increase in the fraction of nonmotile cells at lower inducer concentrations (Fig. 2D). We further confirmed that the class II gene reporter expression reflects the change of filament number (Fig. 4E): Reducing *PfliA-lacZ* level by titrating *flhDC* expression led to a linear drop of the average number of filaments in different growth conditions (Fig. 4E, open symbols). In contrast, the WT strain exhibited little variation in either the filament number or gene expression per cell (Fig. 4E, filled circles). In combination, these findings support the idea that cells regulate motility genes in coordination with cell size such that an average number of flagella per cell is maintained in different growth conditions.

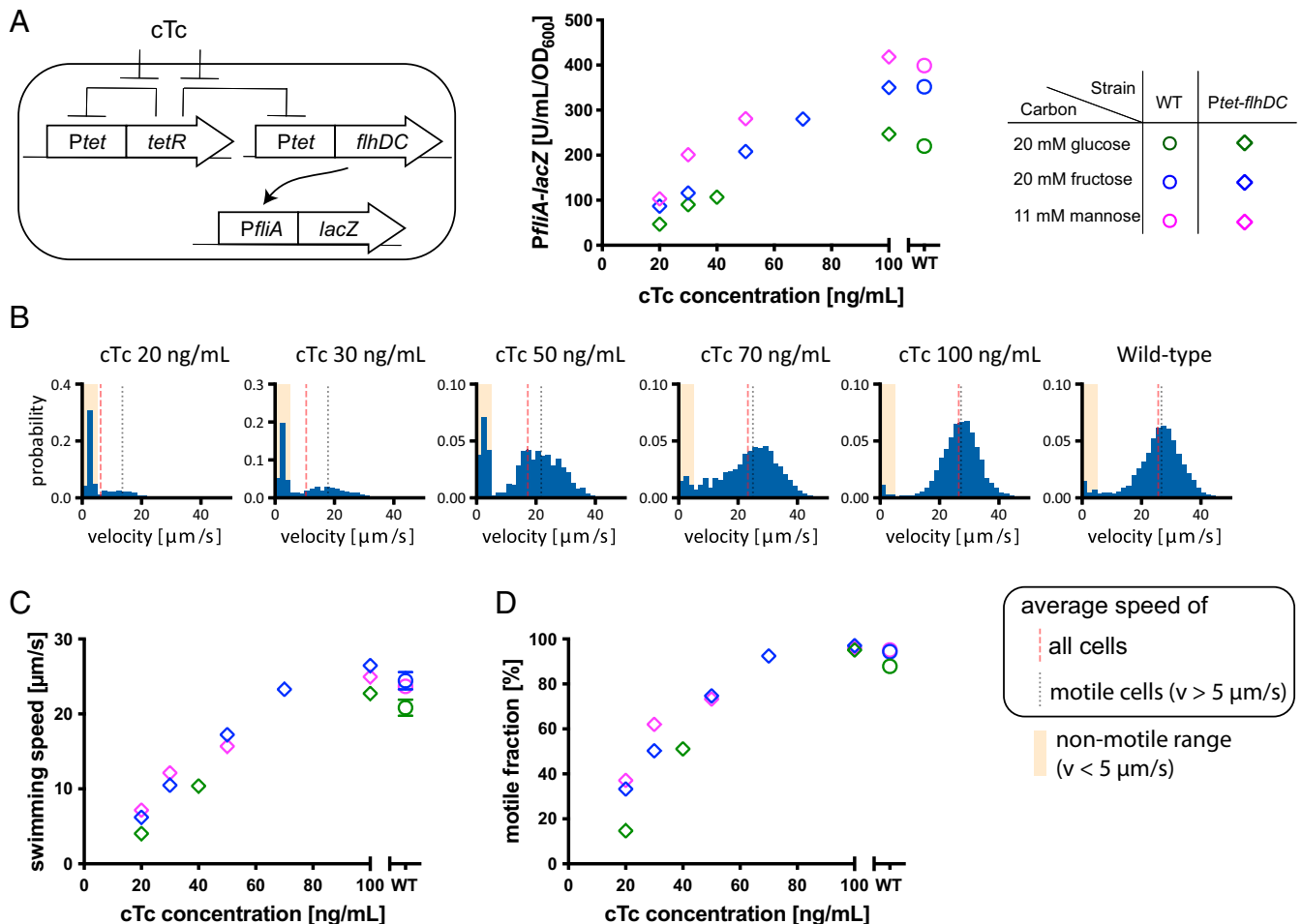


Fig. 2. Gene expression and swimming behavior when titrating a motility master regulator. (A) Titratable *flhDC* construct with *PfiA-lacZ* reporter to quantify *fliA* expression. Titration control is achieved via the *Ptet* system and cTc as inducer. *PfiA-lacZ* expression was measured by varying inducer concentration. (B) Swimming speed distributions when cells are grown on fructose with different inducer levels. (C and D) Changes in average swimming speed and the motile fraction of cells (swimming speed > 5 $\mu\text{m/s}$) in the population. WT is shown as circles in A, C, and D for comparison. Error bars in WT indicate s.d. of biological replicates. Strains HE641 and HE170 were used in A and B–D, respectively (both strains are identical except carrying different *lacZ* reporters: *SI Appendix, Table S1*). The data values are listed in *SI Appendix, Tables S8 and S9*.

To see how efficiently motility genes are regulated, consider the relation between the average number of flagella per cell and the fraction of motile cells (Fig. 4F): When the expression of motility genes is low, such that there are on average less than four flagella per cell (*flhDC* titration with low inducer levels, diamonds), the motile fraction is proportional to the average flagella number (Fig. 4F, gray region: limited motility). In contrast, when expression levels reach close to those of WT, such that there are on average more than four flagella per cell, almost all cells are motile (Fig. 4F, circle points and yellow region: full motility). An even higher expression level per cell would only increase the costs to express extra flagella and was not observed (Fig. 4F, blue region: nonefficient expression). *E. coli* K-12 thus appears to regulate its motility expression levels such that associated resource demands to synthesize and rotate flagella are at the minimum necessary to keep most cells motile. While the requirement for, on average, four flagella per cell ensures that most cells will be motile (yellow region in Fig. 4F), this number is also close to what is minimally required to allow uninterrupted motility when cells halve the number of their flagella during cell division.

Discussion

In this study, we analyzed the regulation of motility genes by *E. coli* in different balanced growth conditions. We found that the

fold change in gene expression per biomass compensates for the variation in cell size, resulting in the average number of flagella per cell remaining constant across growth conditions. This simple regulatory scheme ensures a fully motile population while keeping resource demands to synthesize and rotate flagella to a minimum.

How do cells implement this regulation scheme? Future studies are needed to reveal further mechanistic insights, but our results point to the combined roles of transcriptional and posttranscriptional regulation in determining the abundance of the motility master regulator FlhDC. On the transcriptional level, cAMP-CRP-dependent activation on *flhDC* expression (46, 47) may play an important role, as other cAMP-CRP-dependent genes are known to increase with decreasing growth rates under carbon limitation (27, 48). In addition, the posttranscriptional regulation on *flhDC* expression might further be essential, as we found that modification of the 5'-UTR strongly affected *flhDC* expression. In this context, it is tempting to speculate about the physiological roles of small RNA species, which are being increasingly discovered and found to be involved in diverse regulatory tasks (49, 50). Further, posttranslational regulation on *flhD* via the anti-FlhDC factor (YdiV) might be involved in adjusting the expression of *fliA* and other class II motility genes such that their expression scales with cell size (25).

The findings reported here have implications for bacterial motility from an ecological perspective, particularly concerning its

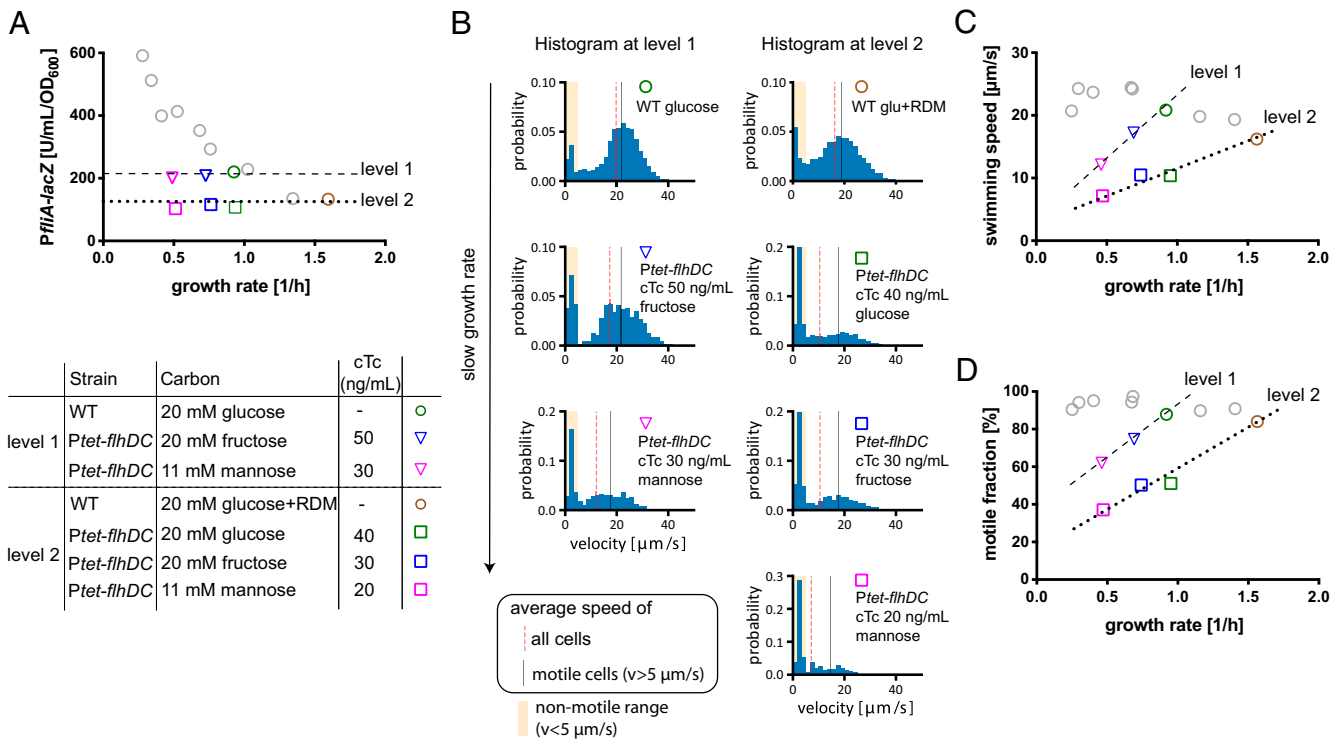


Fig. 3. Swimming behavior across growth conditions at fixed motility expression. (A) *PflIA-lacZ* expression against growth rate when the expression levels are set independent of growth rate by using the titratable *flhDC* construct. To obtain the indicated expression levels, inducer (cTc) concentrations for each growth condition were selected based on the data in Fig. 2A and listed in the legend table. One expression level (level 1, dashed line) resembles the level observed for WT cells growing on glucose (green circle), and the other (level 2, dotted line) resembles the level for WT cells growing on glucose+RDM (brown circle). The other data of *PflIA-lacZ* expression in WT are shown as gray circles for comparison (same data as Fig. 1A). (B) Distributions of swimming speed for the two expression levels (Left column: level 1, Right column: level 2). The fraction of nonmotile cells increases for decreasing growth rate (bars in yellow regions), while the swimming speed of motile cells ($v_i > 5 \mu\text{m/s}$) barely changes (gray lines). The reduction of average swimming with decreasing growth rate (red dotted lines) is thus largely accounted for by the increase of nonmotile fraction. (C and D). The average swimming speed (C) and motile fraction (D) drop for the two fixed expression levels as growth rates decrease (dashed and dotted lines), while WT cells (gray circles, same data as Fig. 1 C and D) exhibit minor changes. Strains HE641 and HE170 were used in A and B–D, respectively. glu, glucose.

role in promoting fitness across different environments. Previous works have highlighted up-regulation as a fingerprint of anticipatory response, with motility triggered when nutrients run out (26, 28–30). In contrast, we here propose that at least a part of the up-regulation of swimming in poorer growth conditions is not a starvation response per se, but an obligatory regulation to maintain sufficiently high flagella numbers and swimming as cell size changes. Future studies are needed to investigate how our findings merge with the ideas of anticipatory response, but the efficient regulation of motility genes to maintain swimming under growth-supporting conditions is in line with observations that bacterial cells quickly stop swimming (9), actively brake motor rotation (51, 52), and even release their flagella upon entering starvation (53, 54). Notably, the maintenance of cellular motility in growth-supporting conditions enables cell population to rapidly expand into unoccupied nutrient-rich territories, boosting overall population growth (9). The growth advantage of such a navigated range expansion relies on cells being motile across conditions, and a delayed onset of motility only in response to starvation would nullify the fitness advantage (9). Therefore, the efficient regulation of motility genes described here does not only minimize the resources required to build and fuel the motility machinery, but it also supports fast navigated range expansion, which further boosts fitness (9, 21, 33).

The findings further provide a perspective on the relation between cell size and growth itself. Throughout the text, we have referred to the change in motility gene expression as an up-regulation in poor nutrient conditions. However, this change can also be viewed as a down-regulation in nutrient-replete conditions

when cells grow fast. Given that the goal of the flagella regulatory system is to maintain the number of flagella per cell, we can view the decreased flagella expression at fast growth also as a consequence of increased cell size at fast growth. This view leads us to suggest a physiological rationale for *E. coli*'s choice of cell size at different growth rates. It is generally preferable for bacterial cells to keep a small biomass (i.e., cell size), as it promotes efficient diffusive transport, fast nutrient uptake, and strong dispersal (55, 56). However, in favorable conditions allowing for rapid growth, the translational machinery per biomass is the most growth-limiting factor (57, 58), and making cell size larger can be beneficial to alleviate this bottleneck: By increasing its size at fast growth, the cell effectively reduces the amount of flagella proteins that need to be synthesized, thus allowing more proteomic resources to be allocated toward ribosomes and other components of the translation machinery. Quantitatively, flagella proteins comprise ~3.0% of the total protein mass in slow carbon-limited conditions and ~0.7% in RDM (11). Thus, by increasing its cell size, *E. coli* manages to “save” 2.3% of the proteome that would have otherwise been tied up in flagella synthesis. To put this amount in perspective, the entire set of biosynthesis enzymes saved when cells are provided with all amino acids and nucleotides is only ~11% of the proteome (comparing the proteome composition of cells grown in rich-defined medium supplemented with glucose to those grown in glucose-minimal medium). This saving accounts for a large share of the increase of growth rate from 1.0 1/h in glucose-minimal medium to 1.8 1/h in RDM (11), based on the well-established linear relation between ribosome content and growth rate, where every percent-of-proteome added to the

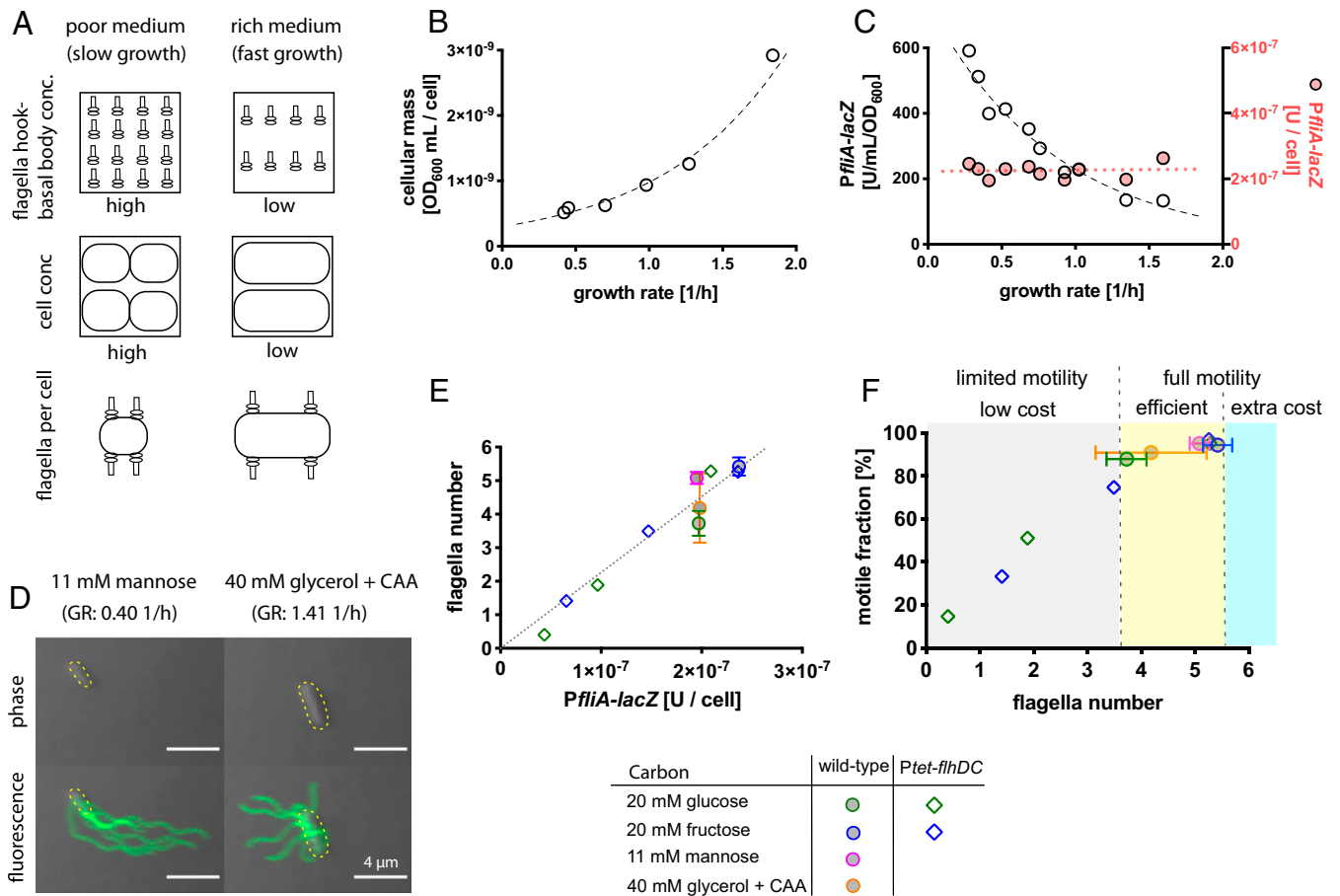


Fig. 4. Expression levels change with cell size such that cells remain motile across growth conditions. (A) The concentration of motility gene products per unit biomass is higher for growth in poor condition (Top), but cells are also smaller when growing more slowly (Middle). Consequently, the abundance of motility gene products expressed per cell, like the number of flagella, would show less variation across growth conditions (Bottom). (B) The average biomass of cells, determined via OD measurements and cell counting (CFU in culture), increases exponentially with growth rate. Line indicates exponential fit, $\sim e^{k\lambda}$, with growth rate λ and parameter $k = 1.18$ 1/h. (C) Expression of the class II gene *fliA* per biomass (open circles) and per cell (red circles) based on the *PflIA-lacZ* measurements (strain HE207). Dashed line shows an exponential fit for the *PflIA-lacZ* expression per biomass, $\sim e^{k\lambda}$ with rate $k = -1.17$ 1/h. The red dotted line indicates the product of the two exponential relations in cell size (B) and *PflIA-lacZ* per biomass. (D) Images of cells with stained flagella filaments in a poor and rich condition (slow and fast growth, Left and Right columns). While cell size differed (phase contrast, Top row), a similar number of flagella filaments was observed (fluorescently labeled filaments, Bottom row). Full distribution across the population is shown in *SI Appendix, Fig. S5*. Yellow lines indicate cell perimeter. (E) Relation between flagella filament number and *PflIA-lacZ* expression per cell for the native (filled circles) and titratable (diamonds) regulation of *flhDC* expression. Line indicates a linear fit with slope $2.26 \cdot 10^7$. Different inducer levels were used for the titratable *flhDC* strain as shown in *SI Appendix, Fig. S6*. (F) Motile fraction and flagella number for WT (circles) and titratable *flhDC* strain (diamonds). WT cells are mostly motile and adjust their expression level per cell to ensure motility (yellow region) while preventing more expression than needed (blue region). Strains HE206 and HE170 were used to obtain swimming data. Strains HE207 and HE641 were used to obtain *PflIA-lacZ* expression data. Flagella filament numbers were quantified using strains HE582 and HE571 harboring a modified *S219C flhC* sequence. Error bars in flagella number of WT indicate s.d. of biological replicates. Cell size data in B from Basan et al. (41). Data values are listed in *SI Appendix, Tables S10 and S11*. CFU, colony formation unit; conc., concentration; GR, growth rate.

protein synthesis machinery results in an ~ 0.06 1/h increase in growth rate (11, 27, 57). Thus, a 2.3% saving in proteome allocation to flagella synthesis would amount to a gain of ~ 0.14 1/h for growth in rich medium. In other words, had *E. coli* kept its size at the level observed in the poor-nutrient condition, then it would suffer a 0.14 1/h reduction in growth rate (from the observed growth rate of 1.8 1/h) in rich medium, just due to motility expression alone. This proteome resource savings by a change of cell size should be similarly applicable to other cellular processes that demand protein expression on a per-cell basis, including cell division and cell pole maintenance. Therefore, increasing cell size at fast growth might be a simple and effective strategy to reduce competition for proteome resources at fast growth, for *E. coli* and possibly many other fast-growing bacterial species.

Materials and Methods

Strains Used in This Study. The reference strain in our study is a motile variant of the *E. coli* K-12 (strain NCM3722B) whose physiology has been well

characterized in previous studies (17, 27, 48, 59, 60). Similar to other motile K-12 strains (61, 62), the strain NCM3722B carries a 1-kb insertion element (IS1) upstream of the *flhDC* transcription site that activates *flhDC* expression and the motile phenotype (46, 63). Detailed information on the strain and derived constructs to report gene expression levels and titrate *flhDC* expression are provided in *SI Appendix, Text 1.1*.

Growth Media. Cells were grown in a modified MOPS-buffered minimal medium (64). Trace micronutrients were not added as the metal components have been reported to inhibit motility (65). To change growth conditions, different carbon sources were provided. When indicated, casamino acids (CAAs) and RDM were additionally provided. When *flhDC* expression was titrated, cTc was provided as an inducer. For the swimming assay and the flagella staining, 0.05% PVP40 was provided to prevent cells and flagella from sticking to material surfaces (66). Additional details on media composition and concentrations are provided in *SI Appendix, Text 1.2.1*.

Strain Culturing and Growth Rate Measurement. Growth measurements were performed in a 37 °C water bath shaker operating at 250 rpm. Each growth experiment was carried out in three steps: seed culture in Luria-Bertani (LB)

broth, preculture, and experimental culture in identical minimal medium. In the seed culture, a single fresh colony from an LB agar plate was inoculated into liquid LB broth and cultured at 37 °C for 4 to 5 h. Cells were then cultured in the specified medium at 37 °C overnight (preculture). The starting OD₆₀₀ in preculture was adjusted so that exponential cell growth was maintained. After preculturing, cells were then diluted to OD₆₀₀ = 0.005 to 0.02 in identical prewarmed medium and grown in a 37 °C water bath shaker (experimental culture). After cells had been grown for at least three generations, OD₆₀₀ was measured around every half doubling of cell growth. About four to six data points below OD₆₀₀ 0.3 were used to calculate growth rate. For cell culturing in rich conditions using CAA and RDM, the experimental cultures were started by diluting saturated precultures and repeating growth and dilution to restore steady-state growth. The cultures were then diluted into fresh medium to start the measurements. Additional details are provided in *SI Appendix, Text 1.2.2*.

Measurements of Swimming Characteristics. To quantify the swimming behavior of cells, samples of 200 µL cell culture were collected at different time points during steady-state growth. Immediately after the collection, samples were diluted to an OD₆₀₀ of ~0.005 using filtered growth medium. The diluted sample was then loaded into a rectangular capillary, and phase-contrast microscopy was used to acquire videos of the swimming cells. A custom-made Python script was then used to obtain cell trajectories and swimming characteristics. Additional details of the experiments and data analysis are provided in *SI Appendix, Text 1.3*. The code is available via GitHub at https://github.com/jonascramer/swimming_analysis.

β-Galactosidase Assay. Samples were collected at different time points during steady-state growth, and β-galactosidase activity was measured by a traditional Miller method. LacZ expression level was determined by taking a linear regression of LacZ activity against OD₆₀₀. Additional details are provided in *SI Appendix, Text 1.4*.

Flagella Number and Length Quantification. Flagella staining was performed by using strains that carry S219C modification in *flhC* sequence. This allowed a direct labeling of flagella filaments by sulfhydryl-specific Alexa Fluor maleimide dyes (67–69). Cell samples were collected at OD₆₀₀ 0.2 during steady state in each condition. Following the washing step, flagella filaments were

labeled by the Alexa Fluor 488 maleimide dye under a dark condition at 37 °C for 15 min. After the excess dye was washed out, cells were imaged between a glass cover and 2% agar pad using a confocal microscope (Leica LSM 8). Fluorophores were excited with a 488-nm laser line, and the detectors were scanned in the wavelength range 500 to 550 nm. Images of 60 to 100 cells were acquired for each experiment. The number of flagella was counted manually, and the length equivalent was determined by dividing the integrated fluorescent signals by the number of flagella for each cell. Additional details of the experiments and data analysis are provided in *SI Appendix, Text 1.5*.

Motor Speed Measurement. A strain carrying sticky-*flhC* was used for the experiment. Cells were collected during steady-state growth, and the flagella were sheared using two syringes connected by a plastic tube. Following the shearing steps, cells were loaded into a flow cell and exposed to a suspension of beads with diameter 0.5 µm. The motor speed was measured via back-focal plane interferometry to track bead rotations (38). Full details of the experiments and data analysis are provided in *SI Appendix, Text 1.6*.

Data Availability. All study data are included in the article and/or supporting information. Previously published data were used for this work (70).

ACKNOWLEDGMENTS. We thank Matteo Mori, Chenhao Wu, and Christina Ludwig for providing proteomic data and Angela Dawson and Ekaterina Krasnopeeva for providing the pTOF24 plasmids carrying S219C and sticky *flhC*. T.Honda acknowledges a JASSO (Japan Student Services Organization) long-term graduate fellowship and JSPS (Japan Society for the Promotion of Science) overseas research fellowship. L.M. and T.P. acknowledge the support of the Cunningham Trust award ACC/KWF/PhD1. Work in the T.Hwa lab is supported by the NIH through Grant No. R01GM109069 and by the NSF through Grant No. MCB 1818384.

Author affiliations: ^aDivision of Biological Sciences, University of California at San Diego, La Jolla, CA 92093; ^bUS Department of Energy, Joint Genome Institute, Berkeley, CA 94720; ^cDepartment of Physics, University of California at San Diego, La Jolla, CA 92093; ^dDepartment of Biology, Stanford University, Stanford, CA 94305; ^eSchool of Biological Sciences, Centre for Synthetic and Systems Biology, University of Edinburgh, Edinburgh, EH9 3FF, United Kingdom; and ^fDepartment of Physics, Cavendish Laboratory, University of Cambridge, Cambridge, CB3 0HE, United Kingdom

1. D. Molenaar, R. van Berlo, D. de Ridder, B. Teusink, Shifts in growth strategies reflect tradeoffs in cellular economics. *Mol. Syst. Biol.* **5**, 323 (2009).
2. H. C. Berg, *E. coli in Motion* (Springer-Verlag, 2004). <https://doi.org/10.1007/b97370> (Accessed 19 April 2021).
3. U. Alon, M. G. Surette, N. Barkai, S. Leibler, Robustness in bacterial chemotaxis. *Nature* **397**, 168–171 (1999).
4. V. Sourjik, N. S. Wingreen, Responding to chemical gradients: Bacterial chemotaxis. *Curr. Opin. Cell Biol.* **24**, 262–268 (2012).
5. A. J. Waite, N. W. Frankel, T. Emonet, Behavioral variability and phenotypic diversity in bacterial chemotaxis. *Annu. Rev. Biophys.* **47**, 595–616 (2018).
6. J. Adler, Chemotaxis in bacteria. *Science* **153**, 708–716 (1966).
7. I. Chet, R. Mitchell, Ecological aspects of microbial chemotactic behavior. *Annu. Rev. Microbiol.* **30**, 221–239 (1976).
8. D. A. Koster, A. Mayo, A. Bren, U. Alon, Surface growth of a motile bacterial population resembles growth in a chemostat. *J. Mol. Biol.* **424**, 180–191 (2012).
9. J. Cremer *et al.*, Chemotaxis as a navigation strategy to boost range expansion. *Nature* **575**, 658–663 (2019).
10. D. W. Erickson *et al.*, A global resource allocation strategy governs growth transition kinetics of *Escherichia coli*. *Nature* **551**, 119–123 (2017).
11. M. Mori *et al.*, From coarse to fine: The absolute *Escherichia coli* proteome under diverse growth conditions. *Mol. Syst. Biol.* **17**, e9536 (2021).
12. D. C. Fung, H. C. Berg, Powering the flagellar motor of *Escherichia coli* with an external voltage source. *Nature* **375**, 809–812 (1995).
13. C. V. Gabel, H. C. Berg, The speed of the flagellar rotary motor of *Escherichia coli* varies linearly with protonmotive force. *Proc. Natl. Acad. Sci. U.S.A.* **100**, 8748–8751 (2003).
14. T. Minamino, Protein export through the bacterial flagellar type III export pathway. *Biochim. Biophys. Acta* **1843**, 1642–1648 (2014).
15. E. J. Gauger *et al.*, Role of motility and the *flhDC* Operon in *Escherichia coli* MG1655 colonization of the mouse intestine. *Infect. Immun.* **75**, 3315–3324 (2007).
16. X. Wang, T. K. Wood, IS5 inserts upstream of the master motility operon *flhDC* in a quasi-Lamarckian way. *J. SME J.* **5**, 1517–1525 (2011).
17. M. Basan *et al.*, Overflow metabolism in *Escherichia coli* results from efficient proteome allocation. *Nature* **528**, 99–104 (2015).
18. X. Yi, A. M. Dean, Phenotypic plasticity as an adaptation to a functional trade-off. *eLife* **5**, e19307 (2016).
19. D. T. Fraebel *et al.*, Environment determines evolutionary trajectory in a constrained phenotypic space. *eLife* **6**, e24669 (2017).
20. B. Ni *et al.*, Evolutionary remodeling of bacterial motility checkpoint control. *Cell Rep.* **18**, 866–877 (2017).
21. W. Liu, J. Cremer, D. Li, T. Hwa, C. Liu, An evolutionarily stable strategy to colonize spatially extended habitats. *Nature* **575**, 664–668 (2019).
22. G. S. Chilcott, K. T. Hughes, Coupling of flagellar gene expression to flagellar assembly in *Salmonella enterica* serovar typhimurium and *Escherichia coli*. *Microbiol. Mol. Biol. Rev.* **64**, 694–708 (2000).
23. S. Kalir *et al.*, Ordering genes in a flagella pathway by analysis of expression kinetics from living bacteria. *Science* **292**, 2080–2083 (2001).
24. D. M. Fitzgerald, R. P. Bonocora, J. T. Wade, Comprehensive mapping of the *Escherichia coli* flagellar regulatory network. *PLoS Genet.* **10**, e1004649 (2014).
25. J. M. Kim, M. Garcia-Alcala, E. Balleza, P. Cluzel, Stochastic transcriptional pulses orchestrate flagellar biosynthesis in *Escherichia coli*. *Sci. Adv.* **6**, eaax0947 (2020).
26. C. D. Amsler, M. Cho, P. Matsumura, Multiple factors underlying the maximum motility of *Escherichia coli* as cultures enter post-exponential growth. *J. Bacteriol.* **175**, 6238–6244 (1993).
27. S. Hui *et al.*, Quantitative proteomic analysis reveals a simple strategy of global resource allocation in bacteria. *Mol. Syst. Biol.* **11**, 784 (2015).
28. B. Ni, R. Colin, H. Link, R. G. Endres, V. Sourjik, Growth-rate dependent resource investment in bacterial motile behavior quantitatively follows potential benefit of chemotaxis. *Proc. Natl. Acad. Sci. U.S.A.* **117**, 595–601 (2020).
29. M. Liu *et al.*, Global transcriptional programs reveal a carbon source foraging strategy by *Escherichia coli*. *J. Biol. Chem.* **280**, 15921–15927 (2005).
30. K. Zhao, M. Liu, R. R. Burgess, Adaptation in bacterial flagellar and motility systems: From regulon members to ‘foraging’-like behavior in *E. coli*. *Nucleic Acids Res.* **35**, 4441–4452 (2007).
31. J. Saragosti *et al.*, Directional persistence of chemotactic bacteria in a traveling concentration wave. *Proc. Natl. Acad. Sci. U.S.A.* **108**, 16235–16240 (2011).
32. X. Fu *et al.*, Spatial self-organization resolves conflicts between individuality and collective migration. *Nat. Commun.* **9**, 2177 (2018).
33. S. Gude *et al.*, Bacterial coexistence driven by motility and spatial competition. *Nature* **578**, 588–592 (2020).
34. N. De Lay, S. Gottesman, A complex network of small non-coding RNAs regulate motility in *Escherichia coli*. *Mol. Microbiol.* **86**, 524–538 (2012).
35. E. Levine, Z. Zhang, T. Kuhlman, T. Hwa, Quantitative characteristics of gene regulation by small RNA. *PLoS Biol.* **5**, e229 (2007).
36. W. S. Ryu, R. M. Berry, H. C. Berg, Torque-generating units of the flagellar motor of *Escherichia coli* have a high duty ratio. *Nature* **403**, 444–447 (2000).
37. E. Krasnopeeva, C.-J. Lo, T. Pilizota, Single-cell bacterial electrophysiology reveals mechanisms of stress-induced damage. *Biophys. J.* **116**, 2390–2399 (2019).
38. J. Rosko, V. A. Martinez, W. C. K. Poon, T. Pilizota, Osmotaxis in *Escherichia coli* through changes in motor speed. *Proc. Natl. Acad. Sci. U.S.A.* **114**, E7969–E7976 (2017).

39. L. Mancini *et al.*, *Escherichia coli*'s physiology can turn membrane voltage dyes into actuators. bioRxiv [Preprint] (2019). <https://doi.org/10.1101/607838>. Accessed 26 October 2020.
40. J. H. Miller, *Experiments in Molecular Genetics* (Cold Spring Harbor Laboratory Press, 1972).
41. M. Basan *et al.*, Inflating bacterial cells by increased protein synthesis. *Mol. Syst. Biol.* **11**, 836–836 (2015).
42. C. L. Woldringh, J. S. Binnerts, A. Mans, Variation in *Escherichia coli* buoyant density measured in Percoll gradients. *J. Bacteriol.* **148**, 58–63 (1981).
43. M. Schaechter, O. MaalØe, N. O. Kjeldgaard, Dependency on medium and temperature of cell size and chemical composition during balanced growth of *Salmonella typhimurium*. *Microbiology* **19**, 592–606 (1958).
44. F. Si *et al.*, Invariance of initiation mass and predictability of cell size in *Escherichia coli*. *Curr. Biol.* **27**, 1278–1287 (2017).
45. H. Zheng *et al.*, General quantitative relations linking cell growth and the cell cycle in *Escherichia coli*. *Nat. Microbiol.* **5**, 995–1001 (2020).
46. K. A. Fahmer, H. C. Berg, Mutations that stimulate flhDC expression in *Escherichia coli* K-12. *J. Bacteriol.* **197**, 3087–3096 (2015).
47. O. Soutourina *et al.*, Multiple control of flagellum biosynthesis in *Escherichia coli*: Role of H-NS protein and the cyclic AMP-catabolite activator protein complex in transcription of the flhDC master operon. *J. Bacteriol.* **181**, 7500–7508 (1999).
48. C. You *et al.*, Coordination of bacterial proteome with metabolism by cyclic AMP signalling. *Nature* **500**, 301–306 (2013).
49. M. K. Mihailovic *et al.*, High-throughput in vivo mapping of RNA accessible interfaces to identify functional sRNA binding sites. *Nat. Commun.* **9**, 4084 (2018).
50. F. De Mets, L. Van Melderen, S. Gottesman, Regulation of acetate metabolism and coordination with the TCA cycle via a processed small RNA. *Proc. Natl. Acad. Sci. U.S.A.* **116**, 1043–1052 (2019).
51. A. Boehm *et al.*, Second messenger-mediated adjustment of bacterial swimming velocity. *Cell* **141**, 107–116 (2010).
52. K. Paul, V. Nieto, W. C. Carlquist, D. F. Blair, R. M. Harshey, The c-di-GMP binding protein YcGR controls flagellar motor direction and speed to affect chemotaxis by a “backstop brake” mechanism. *Mol. Cell* **38**, 128–139 (2010).
53. J. L. Ferreira *et al.*, γ -Proteobacteria eject their polar flagella under nutrient depletion, retaining flagellar motor relic structures. *PLoS Biol.* **17**, e3000165 (2019).
54. X.-Y. Zhuang *et al.*, Live-cell fluorescence imaging reveals dynamic production and loss of bacterial flagella. *Mol. Microbiol.* **114**, 279–291 (2020).
55. A. L. Koch, What size should a bacterium be? A question of scale. *Annu. Rev. Microbiol.* **50**, 317–348 (1996).
56. K. D. Young, The selective value of bacterial shape. *Microbiol. Mol. Biol. Rev.* **70**, 660–703 (2006).
57. M. Scott, C. W. Gunderson, E. M. Mateescu, Z. Zhang, T. Hwa, Interdependence of cell growth and gene expression: Origins and consequences. *Science* **330**, 1099–1102 (2010).
58. M. Scott, S. Klumpp, E. M. Mateescu, T. Hwa, Emergence of robust growth laws from optimal regulation of ribosome synthesis. *Mol. Syst. Biol.* **10**, 747 (2014).
59. E. Soupene *et al.*, Physiological studies of *Escherichia coli* strain MG1655: Growth defects and apparent cross-regulation of gene expression. *J. Bacteriol.* **185**, 5611–5626 (2003).
60. S. D. Brown, S. Jun, Complete genome sequence of *Escherichia coli* NCM3722. *Genome Announc.* **3**, 300879–15 (2015).
61. F. R. Blattner *et al.*, The complete genome sequence of *Escherichia coli* K-12. *Science* **277**, 1453–1462 (1997).
62. J. S. Parkinson, Complementation analysis and deletion mapping of *Escherichia coli* mutants defective in chemotaxis. *J. Bacteriol.* **135**, 45–53 (1978).
63. C. S. Barker, B. M. Prüss, P. Matsumura, Increased motility of *Escherichia coli* by insertion sequence element integration into the regulatory region of the flhD operon. *J. Bacteriol.* **186**, 7529–7537 (2004).
64. S. Cayley, M. T. Record Jr., B. A. Lewis, Accumulation of 3-(N-morpholino)propanesulfonate by osmotically stressed *Escherichia coli* K-12. *J. Bacteriol.* **171**, 3597–3602 (1989).
65. J. Adler, B. Templeton, The effect of environmental conditions on the motility of *Escherichia coli*. *Microbiology* **46**, 175–184 (1967).
66. H. C. Berg, L. Turner, Chemotaxis of bacteria in glass capillary arrays. *Escherichia coli*, motility, microchannel plate, and light scattering. *Biophys. J.* **58**, 919–930 (1990).
67. L. Turner, R. Zhang, N. C. Darnton, H. C. Berg, Visualization of flagella during bacterial swarming. *J. Bacteriol.* **192**, 3259–3267 (2010).
68. L. Turner, A. S. Stern, H. C. Berg, Growth of flagellar filaments of *Escherichia coli* is independent of filament length. *J. Bacteriol.* **194**, 2437–2442 (2012).
69. L. Turner, H. C. Berg, “Labeling bacterial flagella with fluorescent dyes” in *Bacterial Chemosensing: Methods and Protocols, Methods in Molecular Biology*, M. D. Manson, Ed. (Springer, 2018), pp. 71–76.
70. M. Mori, *et al.*, From coarse to fine: The absolute *Escherichia coli* proteome under diverse growth conditions. *Mol. Syst. Biol.* **17**, e9536 (2021).